Artificial Intelligence for Engineering Design, Analysis and Manufacturing

www.cambridge.org/aie

Design of an intelligent simulator ANN and ANFIS model in the prediction of milling performance (QCE) of alloy 2017A

Kamel Bousnina, Anis Hamza and Noureddine Ben Yahia

Higher National Engineering School of Tunis (ENSIT), University of Tunis, Mechanical, Production and Energy Laboratory (LMPE), Avenue Taha Hussein, Montfleury, 1008 Tunis, Tunisia.

Research Article

Cite this article: Bousnina K, Hamza A and Yahia NB (2024). Design of an intelligent simulator ANN and ANFIS model in the prediction of milling performance (QCE) of alloy 2017A. *Artificial Intelligence for Engineering Design, Analysis and Manufacturing*, **38**, e23, 1–18
https://doi.org/10.1017/S089006042400009X

Received: 14 January 2023
Revised: 25 May 2023
Accepted: 20 June 2024

Keywords:
Machining strategies; Energy consumption; Machining cost; Surface quality; ANN; ANFIS

Corresponding author:
Anis Hamza;
Email: anis7amza@gmail.com

Abstract

Artificial neural networks (ANNs) and adaptive neuro-fuzzy inference systems (ANFISs) are machine learning techniques that enable modeling and prediction of various properties in the milling process of alloy 2017A, including quality, cost, and energy consumption (QCE). To utilize ANNs or ANFIS for QCE prediction, researchers must gather a dataset consisting of input–output pairs that establish the relationship between QCE and various input variables such as machining parameters, tool properties, and material characteristics. Subsequently, this dataset can be employed to train a machine learning model using techniques like backpropagation or gradient descent. Once the model has been trained, predictions can be made on new input data by providing the desired input variables, resulting in predicted QCE values as output. This study comprehensively examines and identifies the scientific contributions of strategies, machining sequences, and cutting parameters on surface quality, machining cost, and energy consumption using artificial intelligence (ANN and ANFIS). The findings indicate that the optimal neural architecture for ANNs, utilizing the Bayesian regularization (BR) algorithm, is a {3-10-3} architecture with an overall mean square error (MSE) of 2.74×10^{-3}. Similarly, for ANFIS, the optimal structure yielding better error and correlation for the three output variables (E_{tot}, C_{tot}, and Ra) is a {2, 2, 2} structure. The results demonstrate that using the BR algorithm with a multi-criteria output response yields favorable outcomes compared to the ANFIS.

Introduction

The manufacturing sector is one of the world's largest consumers of electrical energy. With the increase in the cost of energy and the associated carbon emissions, reducing energy demand has become an urgent challenge for manufacturers in recent years. The machine tool consumes a great deal of electrical energy. With the aim of reducing energy consumption and cost in CNC machining, the selection of optimal machining strategies and cutting parameters is considered one of the most important saving policies. The use of new prediction and optimization techniques with artificial intelligence technology can positively contribute to this economic policy. Several researchers have used artificial intelligence tools to solve prediction and optimization problems in mechanical manufacturing. Ben Yahia et al. [1] have developed an integrated environment for the automated planning of machining processes to fabricate prismatic parts. The system is based on the application of the neural network. The system presented is based on the application of the ANN. The model used in this study is applied to the design of the features, namely pockets, grooves, steps, and essentially their intersections: pocket/pocket, step/pocket, step/step, pocket/groove, step/groove, and groove/groove. Girish and Kuldip [2] used the neural network (NN) to predict energy consumption and surface roughness (Ra). They performed machining experiments to verify the suitability of the proposed model for predicting energy consumption and Ra. The results predicted by the proposed model indicate a good synchronism between the predicted values and the values. Aykut et al. [3] studied the milling Ra of alloy AA6061. An experimental model has been improved to assess surface quality using response surface methodology (RSM) and artificial neural networks (ANNs). Serra et al. [4] used multi-objective optimization by the genetic algorithm (GA) by integrating regression analysis to simultaneously minimize Ra, power consumption, and cutting time and maximize productivity. Tzu-Liang et al. [5] developed a Ra prediction model for a set of input data, namely cutting speed, cutting depth, and feed rate. The model was verified by comparing the fuzzy output (FL) with the experimental data used to build the empirical model. The results of these experiments are in good agreement with those predicted by the fuzzy logic model.

In mechanical manufacturing, machine tools consume energy that can reach critical values. Improving the energy efficiency of machine tools can lead to a significant reduction in the cost of products. Research on reducing energy consumption is still insufficient in view of the increasing use of energy sources [6]. For example, Yansong et al. [7] presented an approach that

integrates both Ra and energy consumption to optimize cutting parameters during turning. Ampara and Paul [8] studied how different tool paths can influence the direct energy demand in machining. Therefore, they suggested a way to drastically reduce the energy intensity at the level of material removal. Experimentation demonstrates that the energy consumption of the unidirectional method for the *y* axis, about 230 kWh, is more than that of the parallel contour, 120 kWh. Resul et al. [9] presented a prediction model to estimate the energy consumption involved in milling prismatic parts. They studied the effect of the cutting strategy on the energy consumed and the total cutting time of the rectangular open pocket feature. Measurements of cutting energy, auxiliary energy, and base energy showed that the "zigzag" cutting strategy consumes the least energy, and the "zig with contour" strategy consumes more energy. Congbo et al. [10] carried out a set of experiments to demonstrate the performance of operational strategies in the milling process. The authors used five tool path strategies in this process, namely bidirectional along x, parallel contour, bidirectional along y, bidirectional at an angle of 45 °, and spiral contour. The results showed that the maximum specific energy consumed (SEC) is given by the strategy of the spiral contour (87 J/mm^3). On the other hand, the minimum energy is given by the bidirectional strategy along *x* (53.1 J/mm^3). In the work of Bousnina and Hamza [6], the authors studied the effects of cutting parameters on energy consumption in the turning process of 304-L stainless steel. These studies have shown that the reduction in energy consumption can reach a value of 58.42%. They also showed that the increase in the energy efficiency (EE) of the machine can reach 18.96%.

Few researchers have evaluated optimal cutting conditions based on minimum cost during the manufacturing process. For example, Qiulian et al. [11] used multi-objective optimization by the non-dominated sorting genetic algorithm II (NSGA-II) algorithm oriented toward three objectives and affected by three variables. The three variables are feed rate, depth of cut, and cutting speed. The three goals are energy consumption, minimum machining cost, and better Ra. Congbo et al. [12] studied multi-pass milling face milling and used multi-objective optimization to maximize energy efficiency and minimize production costs by the adaptive multi-objective particle swarm. The results showed that increasing cutting speed, depth of cut, and feed rate simultaneously reduced production time and cost. To achieve energy saving and low cost of CNC machining, Yongmao et al. [13] used a multi-objective optimization approach by integrating the adaptive particle swarm optimization (APSO) algorithm and the improved GA (NSGA-II). Experimental results have shown that the multi-objective optimization model is feasible and efficient and that it can effectively help operators balance energy consumption and manufacturing costs.

Optimizing this process has become a primary stake to reach higher productivity and quality. To optimize process planning, it is important to select a suitable machining strategy [14]. The main objective of this research is to provide a multi-criteria help tool for determining the optimal machining process by integrating the factors: QCE.

The inventory of the main works of research on the optimization of the machining process shows the wide variety of tools and parameters that can influence this process. Table 1 presents these different works. This table shows that these studies are devoted mainly to the definition of simple machining entities (facing, pocket, etc.). On the other hand, most of these studies use some strategies without taking into account the machining ranges (sequences). It was also found that the influence of machining strategies and sequences on the manufacturing cost is nonexistent in all previous studies. On the other hand, the combination of the roughness, cost, and energy output responses is linked only with the cutting parameters and this is for the work of Qiulian et al. [11].

Finally, there is no study or model that takes into account cutting parameters, strategies, and machining ranges at the same time for the modeling and optimization of surface quality, machining cost, and energy consumed (QCE) of numerically controlled machine tools to machine interacting entities using artificial intelligence, which will be the subject of this article.

Table 1. The different works presented

	Input			Output			
Ref.	Cutting parameters	Strategies	Sequences	Surface quality	Energy	Cost	Methods
Ben Yahia et al. [1]			✓				ANN
Girish and Kuldip [2]	✓			✓			ANN, FL, MR, GA
Aykut et al. [3]	✓			✓			ANN, RSM
Serra et al. [4]	✓			✓	✓		MLR, GA
Tzu-Liang et al. [5]	✓			✓			LF
Yansong et al. [7]	✓			✓	✓		-
Ampara and Paul [8]	✓	✓			✓		Mod
Resul et al. [9]	✓	✓			✓		RSM
Congbo et al. [10]	✓	✓			✓		-
Bousnina and Hamza [6]	✓				✓		RSM
Qiulian et al. [11]	✓			✓	✓	✓	NSGA-II
Congbo et al. [12]	✓				✓	✓	AMOPSO
Yongmao et al. [13]	✓				✓	✓	APSO, NSGA-II
This work	✓	✓	✓	✓	✓	✓	**GRA, ANN, ANFIS**

https://doi.org/10.1017/S089006042400009X Published online by Cambridge University Press

Experimental methods

The main objective of manufacturing industries is to minimize the cost of the finished product as much as possible while maintaining the superior quality of the product. Today, energy consumption has become the main factor that directly influences the cost of machining. Faced with this problem, it is necessary to minimize the energy consumption of machine tools in the machining process. This minimization cannot be obtained without knowing all the machining strategies. The problem gets a bit more complicated when we talk about interacting machining features. Figure 1 depicts aeronautical structural parts that are required for frame construction and are frequently manufactured using numerically controlled machine tools. These parts are high-value critical components full of complex and interactive machining features, for example, hole/pocket and pocket/groove.

Most researchers who have worked on energy consumption use a single machining feature, for example, pocket and surfacing, with a limited number of tool paths. Under these conditions, it is difficult to measure this consumption since a part can contain several features and these features can interact, which requires several combinations of machining operations. So the contribution in this work is made there, that is, by creating several sequences (ranges) with different machining strategies in order to choose the optimal sequence that gives minimum cost, energy consumption, and roughness. A machining strategy is a methodology used to generate a series of operations to produce a given shape. The choice of these strategies will be to achieve well-determined specifications and shapes. In this context, three machining strategies have been chosen (zigzag, zig, and inward parallel contour (IPC); Figure 2.

In this part, the case of pocket/groove features has been studied by illustrating the effects of the planning of machining sequences, machining strategies, and cutting parameters on the surface quality, manufacturing cost, and energy. Figure 3 presents the machining features associated with the selected part. In order

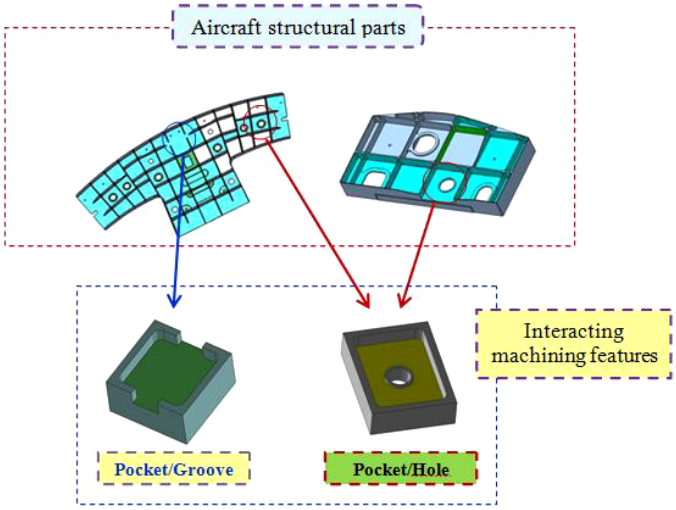

Figure 1. Example of interacting machining features of aircraft structural parts [15].

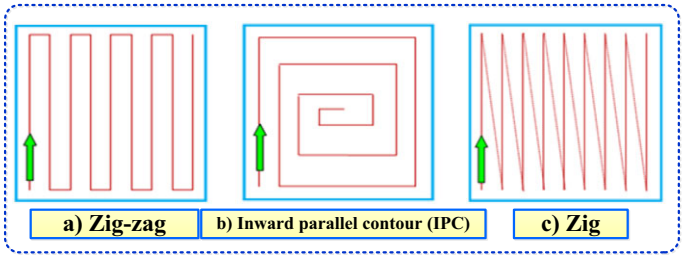

Figure 2. Machining strategies.

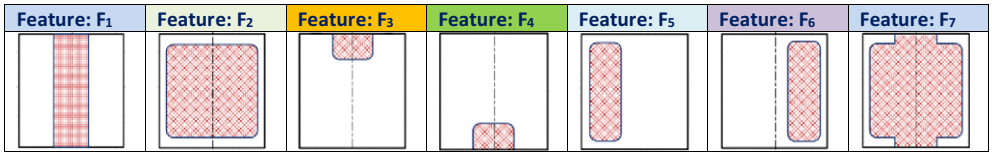

Figure 3. Machining features.

https://doi.org/10.1017/S089006042400009X Published online by Cambridge University Press

Table 2. Machining sequences

No.	Machining sequences (S_i)	Machining features (F_i)	Machining strategies
1	S_1	F_1-F_2	IPC-IPC
2	S_2	F_2-F_1	IPC-IPC
3	S_3	F_3-F_2-F_4	IPC-IPC-IPC
4	S_4	F_2-F_3-F_4	IPC-IPC-IPC
5	S_5	F_1-F_2	Zigzag–IPC
6	S_6	F_2-F_1	IPC-zigzag
7	S_7	F_1-F_2	Zig-IPC
8	S_8	F_1-F_5-F_6	IPC-IPC-IPC
9	S_9	F_2-F_1	IPC-zig
10	S_{10}	F_2-F_3-F_4	IPC-zigzag-zig
11	S_{11}	F_1-F_5-F_6	Zig-IPC-IPC
12	S_{12}	F_1-F_5-F_6	Zigzag-IPC-IPC
13	S_{13}	F_7	IPC

to make this part, the machining features will be used to finally obtain a set of combinations of sequences called the "machining range." Table 2 illustrates all the machining sequences used in this study with the different combinations of strategies (zigzag, IPC, and zig).

Materials and measurements

All the experimental tests are carried out at the workshops at the Higher Institute of Technological Studies of Gabes (ISET Gabes). The machine used is a Realmeca C300H 4-axis machining center. The center generates power between 5.5 kW and 7.5 kW with a maximum rotation frequency of 6500 rpm. This machine is powered by 380 V electrical energy and 6 bar pneumatic energy. The Catia V5 software used in this work makes it possible to create the tool paths and then generate the G-code program compatible with the Num director of the center. The tool used is an uncoated high-speed steel tool with a diameter of 8 mm and two teeth (Figure 4).

The material of the machined part is an aluminum alloy (2017A: AlCu4MgSi). This material is widely used in the aerospace, automotive, and so forth industries. This material has high mechanical characteristics after treatment and also good machinability, polishability, and good heat resistance between 100 and 250 °C. Table 3 shows the chemical composition of the material used.

A Chauvin-Arnoux CA8332 power analyzer was used in order to measure the power consumed by the machine at each instant during a machining operation. Data processing is performed using the Power Analyzer's Dataview interface. Figure 5 illustrates the shape of the power consumed during the machining of the S_6 sequence. This graph consists of two main parts. The first part is the machining of the features F_2 with the IPC strategy, which in turn consists of three practically identical parts which correspond to the three layers of the same depth of cut (a_p). Also, note that each layer consists of a pace for a cutting width a_e = tool diameter and a second for a width a_e = 3 mm. This is why the power for the first width is greater than the second. Now for the second part, the tool, after completing the first feature F_2, will move on to execute F_1. During the machining of F_1, the tool, a large part of its trajectory passes empty (without cutting) because a large part of the material has been removed by the feature F_2. For this, the machining phase of this part is practically nonvisual in the shape of the power.

According to Figure 5, the power consumed can be written in the following forms:

$$P_{pi} = P_0 + P_{c\_pi} \quad i = \text{the th layer} \quad 1 \leq i \leqslant 3 \tag{1}$$

$$P^*_{pi} = P_0 + P^*_{c\_pi} \tag{2}$$

$$P_g = P_0 + P_{c\_g} \tag{3}$$

The arithmetic Ra is measured using a KR100 roughness meter. The stroke measured is 6 mm for a caliber of 2.5 mm. Two studies will be carried out in order to reduce energy consumption, minimize the cost of machining, and increase the surface quality of the machined part. The working method for the first case study consists of carrying out a set of machining sequences with different strategies while keeping the cutting parameters constant, namely cutting speed, feed rate, and depth of cut. This is in order to see the influence of sequences and machining strategies on energy consumption, cost, and surface quality. Following and after the realization of the first case and the prediction of the optimal sequence by the use of gray relational analysis (GRA), an experimental plan with a variation of the cutting parameters on this sequence will be carried out in the second case. The objective, in this case, is to predict the experimental results by the use of artificial intelligence and to determine the effects of the cutting parameters on the output responses. The work plan is shown in Figure 6.

One of the big problems in companies is determining the time and cost of manufacturing a product [16]. In the case of CNC machining, it is also interesting to determine the time and cost of each operation in order to choose the optimal machining sequence which takes into account QCE in its execution. The cost of a machining operation can be estimated by the equation:

$$C_{tot} = C_{Machine} + C_{Tool} + C_{Energy} \tag{4}$$

$$C_{Machine} = \mu_1 + t_{cycle} \cdot \mu_2 \tag{5}$$

$$C_{Tool} = \varepsilon \frac{t_c}{T} \tag{6}$$

$$C_{Energy} = \delta E_{tot} \tag{7}$$

Results and discussion

CNC machines are the most important means of production in the manufacturing industry that consumes a large amount of energy during a machining operation. A presentation of the results of the two case studies will be carried out in this part.

First case

The first case study focuses on the variation of machining strategies and sequences by setting the cutting parameters for all the tests. The choice of technological machining parameters was made taking into account the catalog of the tool manufacturer and the capacity of the machining center. Table 4 presents the cutting parameter values used in this first part. This study takes into consideration the machining sequences and strategies (tool paths) in order to obtain the optimal sequence. Table 5 illustrates the values of energy consumed, cost, and roughness. Table 6 presents the energy

https://doi.org/10.1017/S089006042400009X Published online by Cambridge University Press

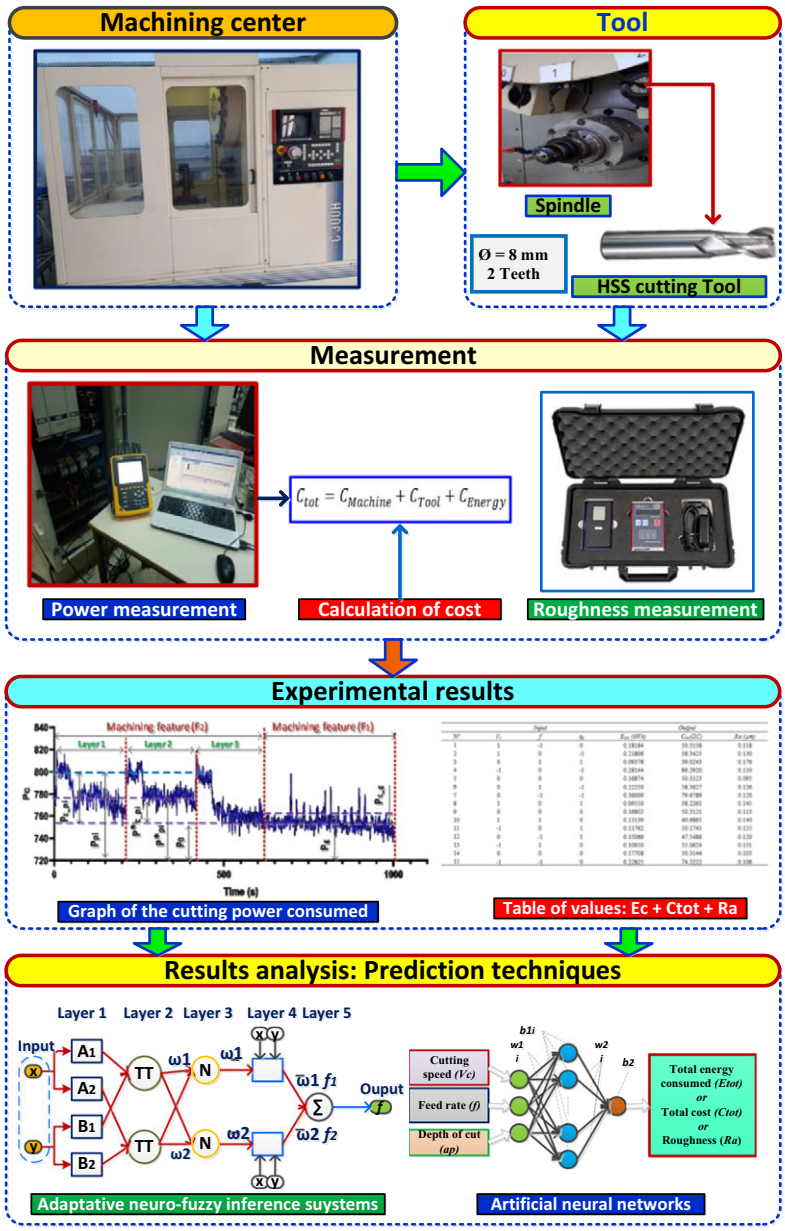

Figure 4. Measurement plan.

Table 3. Chemical composition of the material (wt%)

Si	Fe	Cu	Mn	Mg	Cr	Zn	Al
0.20 à 0.80	Max 0.7	3.5 à 4.5	0.40 à 1	0.40 à 1	0.1	0.25	The rest

consumed for feature F1 for the different strategies (IPC, zigzag, and zig). Figure 7 illustrates the effects of each strategy for this feature F_1 on the energy consumed (E_{tot}). The figure shows that the IPC strategy admits minimum energy consumption compared to the other two. The maximum energy consumption for F_1 is achieved with the zig strategy. This increase in energy for this strategy means that the cut is done in one direction and that the tool for a significant part of its cycle moves in the air. This conclusion converges with the results of Edem et al. [17] and Altıntaş et al. [18]. Figure 8 illustrates graphs of energy consumed and machining cost. The figure shows that the two graphs follow the same variation, which proves that the energy consumed has a significant influence on the cost. As a result, good energy policy management in industries allows for cost reductions in manufacturing. On the other hand, the sequence $S_8 = F_1\text{-}F_5\text{-}F_6$ has the minimum cost and energy. This sequence is characterized by the fact that the tool along its trajectory is in full material (cutting phase). In other words, the tool along its trajectory does not cross empty areas (without material). This condition saves a significant amount of cutting time. On the other hand, the S_8 sequence is realized by the IPC strategy for all the features $F_1\text{-}F_5\text{-}F_6$, which proves that the choice of the tool path and the machining sequence has a significant influence on the cost and energy.

Industry and researchers face a big challenge when they try to study the surface quality of machined parts. Most researchers who

https://doi.org/10.1017/S089006042400009X Published online by Cambridge University Press

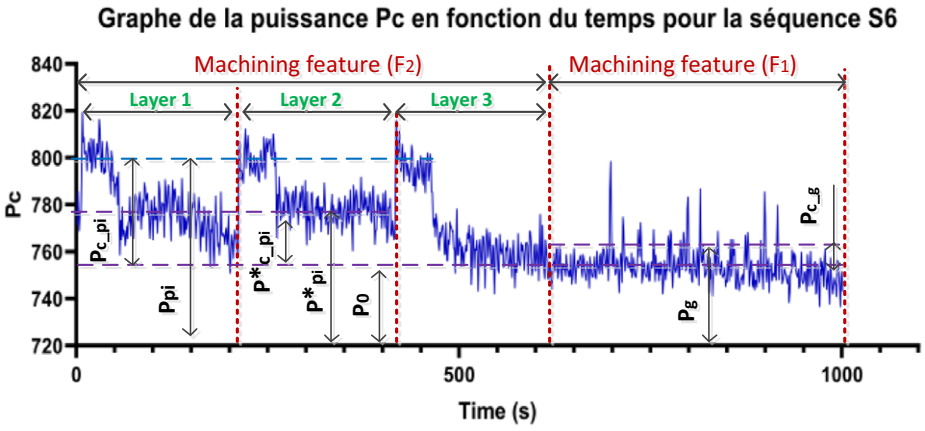

Figure 5. Graph of the power consumed for the sequence S_6.

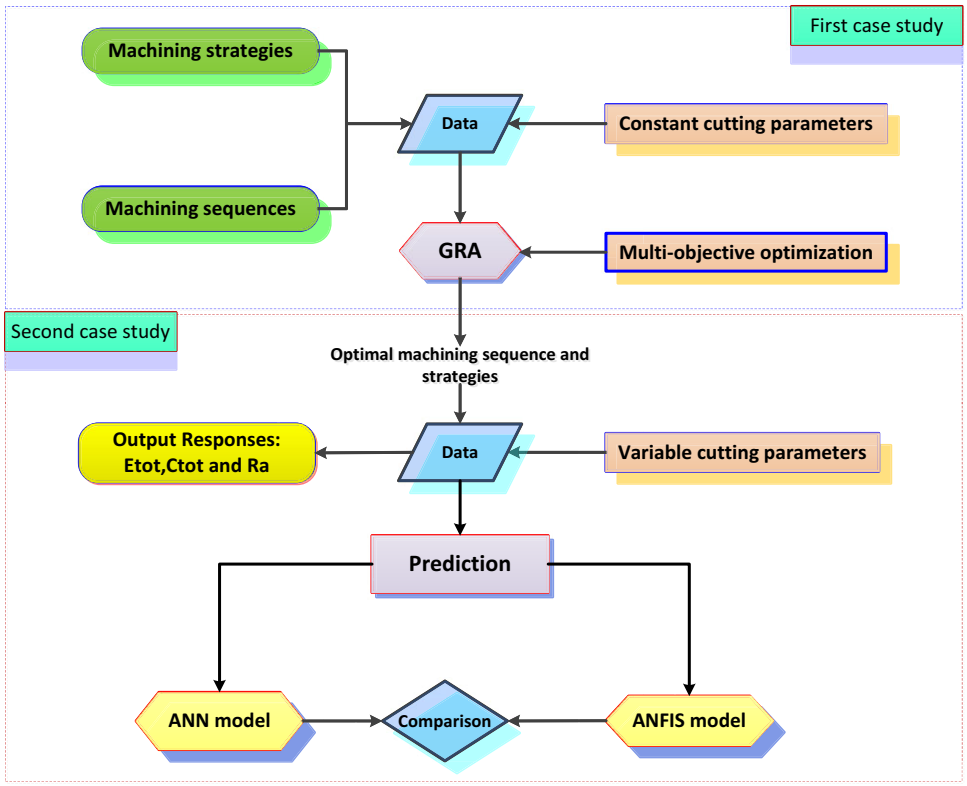

Figure 6. Work plan diagram.

Table 4. Cutting parameters (first case)

V_c (m/min)	N (rev/min)	a_p (mm)	f (mm/rev)	V_f (mm/min)
50	2000	0.5	0.1	200

have worked on surface quality as a function of the tool path have used a single machining feature in their studies. Examples of this claim are the work of Zaleski et al. [19] and Ali Raneen et al. [20]. Indeed, the use of interacting features with a set of tool paths can lead to logic of the choice of surface quality. On the other hand, an overlay of tool paths when machining Fi features can modify the surface texture of the machined part.

Figure 9 shows the Ra of successive machining of F_1-F_2 entities for sequences S_1, S_5, and S_7 with IPC-IPC, zigzag-IPC, and zig-IPC strategies, respectively. The figure shows that machining F_1 and then F_2 (F_1-F_2) with zig-IPC strategies has the lowest roughness. According to the references by Aramcharoen et al. [21] and Ali Raneen et al. [20], the zig strategy for machining a single feature has the maximum roughness compared to the IPC strategy, which has the lowest roughness. In this study, the problem is a little different since the tool for the first feature F_1 creates several passes with the same strategy in order to complete the depth h of the part. Then, the tool will switch to executing F_2 with another strategy. The problem occurs in the last pass for feature F_2. Indeed, the tool causes the last pass with this new strategy, which passes over the texture left by the

https://doi.org/10.1017/S089006042400009X Published online by Cambridge University Press

Table 5. Experimental values (first case)

No.	(S_i)	Machining features (F_i)	Machining strategies	E_{tot} (kWh)	C_{tot} (TD)	Ra (μm)
1	S_1	F_1-F_2	IPC-IPC	0.188	51.328	0.141
2	S_2	F_2-F_1	IPC-IPC	0.194	52.298	0.155
3	S_3	F_3-F_2-F_4	IPC-IPC-IPC	0.159	47.506	0.120
4	S_4	F_2-F_3-F_4	IPC-IPC-IPC	0.168	47.508	0.103
5	S_5	F_1-F_2	Zigzag-IPC	0.205	53.664	0.131
6	S_6	F_2-F_1	IPC-zigzag	0.202	53.653	0.163
7	S_7	F_1-F_2	Zig-IPC	0.269	63.976	0.090
8	S_8	F_1-F_5-F_6	IPC-IPC-IPC	0.135	44.956	0.101
9	S_9	F_2-F_1	IPC-zig	0.265	64.003	0.115
10	S_{10}	F_2-F_3-F_4	IPC-zigzag-zig	0.197	52.360	0.128
11	S_{11}	F_1-F_5-F_6	Zig-IPC-IPC	0.220	56.665	0.153
12	S_{12}	F_1-F_5-F_6	Zigzag-IPC-IPC	0.149	46.322	0.118
13	S_{13}	F_7	IPC	0.149	46.383	0.131

Table 6. The energy consumed for machining the feature (F_1) with the different strategies (first case)

	E_{tot} (kWh)		
Features	IPC	Zigzag	Zig
F_1	0.0559	0.0669	0.1390

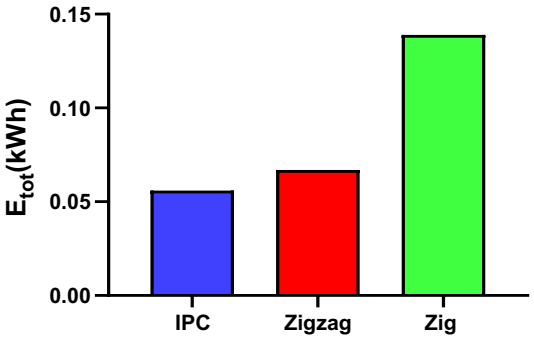

Figure 7. Histogram of the energy consumed for feature (F_1) with the different strategies.

first strategy of the feature F_1. This phenomenon can cause a superfinish in the F_1 area. This is possible when the first strategy has a poor surface quality compared to the second strategy. The conclusion of Aramcharoen et al. [21] that there is a synergy between the roughness and the energy consumed is not valid in this study because the problem is more complicated given that the tool makes trajectories in the air (without cutting), which can disturb this conclusion, which is not the case in the studies by Aramcharoen et al. [21] and Ali Raneen et al. [20]. The next step is to determine the optimal sequence S_i, which gives minimum energy consumption, machining cost, and Ra.

Multi-objective optimization by GRA

After carrying out the experimental tests for this first case, it is now necessary to determine the optimal machining sequence. In this study, there are three output responses, namely energy consumed, cost, and roughness. In this case, it is necessary to have a tool capable of solving this multi-criteria optimization problem. GRA helps to solve this type of uncertainty problem given its ability to understand uncertain systems with partially known information [22]. This theory was established by Deng in the late 1990s. The procedure required by this theory is presented as follows [20]: To

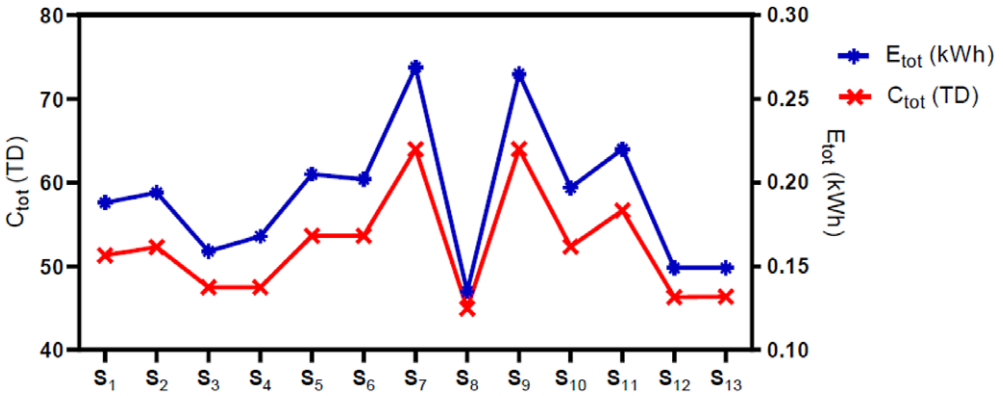

Figure 8. Energy and cost graphs for all sequences.

https://doi.org/10.1017/S089006042400009X Published online by Cambridge University Press

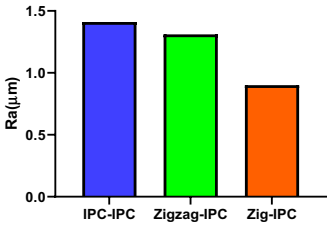

Figure 9. Surface roughness histogram of F_1-F_2 features made with IPC-IPC, zigzag-IPC, and zig-IPC strategies.

obtain better surface quality, minimum cost, and low power consumption, the condition "the lower the better" will be chosen.

$$x_i = \frac{max\, y_i(k) - y_i(k)}{max\, y_i(k) - min\, y_i(k)} \tag{8}$$

where x_i is the output response after normalization and $y_i(k)$ is the experimental values of the output responses. The largest and smallest values are $\max(y_i(k))$ and $\min(y_i(k))$, respectively.

After normalization, the next step is devoted to the calculation of the gray relational coefficient (GRC). The following equation presents this coefficient:

$$\psi_i = \frac{\Delta_{min} + \phi\Delta_{max}}{\Delta_{0i}(k) + \phi\Delta_{max}} \tag{9}$$

where $\Delta_{0i}(k)$ represents the absolute value of the deviation between the test reference $y_0(k)$ and $y_i(k)$, $\Delta_{0i}(k) = \|y_0(k) - y_i(k)\|$. Δ_{min} and Δ_{max} respectively represent the minimum and maximum value of $\Delta_{0i}(k)$. ϕ represents the distinctive coefficient which includes the interval [0,1]. In this work, the coefficient ϕ is 0.5.

The next step is to figure out the gray relational grade (GRG) after figuring out the GRC.

$$\gamma_i = \sum_{k=1}^{n} \omega_k \psi_i \tag{10}$$

where ω_k denotes the normalized weight of the kth experimental response.

In the methodology of GRA, the maximum value of γ_i indicates that the input parameters associated with this value are close to the optimum [23]. In this work and according to Table 7, the maximum value of γ_i corresponds to the sequence S_8. This sequence shows the best way to combine the input parameters, taking into account their different weights. In this first study, the cutting parameters are constant for all the tests, so the combination F_1-F_5-F_6 with the same IPC machining strategy is the optimal combination.

In what follows, the study relates to this sequence S_8 with the combination F_1-F_5-F_6.

Second case

In this second part, the objective is to determine the effects of the cutting parameters on the output variables, E_{tot}, C_{tot}, and Ra. Predicting experiment results has been done by using neural networks (ANNs) and adaptive neuro-fuzzy inference systems (ANFISs). The last phase of this second part is a comparison between the two artificial models in order to choose the model that gives more refined results. The cutting parameters associated with this part are shown in Table 8.

Table 7. Gray relational grade (GRG) (first case)

Si	ψ_i			γ_i	Rank
	E_{tot}	C_{tot}	Ra		
S_1	0.56	0.60	0.42	0.525	6
S_2	0.53	0.56	0.36	0.485	9
S_3	0.74	0.79	0.55	0.691	5
S_4	0.67	0.79	1.00	0.820	2
S_5	0.49	0.52	0.47	0.494	8
S_6	0.50	0.52	0.33	0.452	10
S_7	0.33	0.33	0.66	0.442	11
S_8	**1.00**	**1.00**	**0.74**	**0.912**	**1**
S_9	0.34	0.33	0.59	0.422	12
S_{10}	0.52	0.56	0.49	0.524	7
S_{11}	0.44	0.45	0.37	0.419	13
S_{12}	0.83	0.87	0.57	0.756	3
S_{13}	0.83	0.87	0.47	0.723	4

Table 8. Cutting parameters (second case)

Factors	Levels		
	−1	0	1
V_c (m/min)	25.3	37.69	50.26
f (mm/rev)	0.075	0.1	0.125
a_p (mm)	0.3	0.5	0.75

The depth of cut (a_p) is chosen to ensure that for each level, the tool removes the same depth. The total cutting height of the part is $h = 1.5$ mm. Table 9 presents the experimental values of the 15 trials of E_{tot}, C_{tot}, and surface quality for the machining of the S_8 sequence with a different combination of cutting parameters.

Prediction with ANN

ANN models are programming techniques that simulate the human brain [24]. These models have been implemented in several manufacturing, scheduling, and other industry applications [25]. An ANN is a digital adoption composed of manipulation (processing) elements called neurons. Neurons form a complex random system that generates a relationship between input parameters and output variables. Nonlinear regression analysis of network output responses [26] is used to figure out how well neural network-based predictions work. In general, NN consists of three layers, input layers, hidden layers, and output layers.

Two proposals for neural architecture were presented in this study in order to determine the structural performance of a neural network. The first architecture consists of three inputs (V_C, f, and a_p) and three outputs (E_{tot}, C_{tot}, and Ra) at the same time (Figure 10a). The second consists of three inputs and a single output presented by the networks ANN1, ANN2, and ANN3 (Figure 10b).

The objective of this study is to determine the optimal structure at the output level, number of hidden neurons, and level of the learning algorithm used. The performance of all structures is measured using the MSE during the algorithm learning process. The MSE is given by the following equation:

https://doi.org/10.1017/S089006042400009X Published online by Cambridge University Press

Table 9. Experimental values (second case)

No.	Input			Output		
	V_c	f	a_p	E_{tot} (kWh)	C_{tot}(DT)	*Ra* (µm)
1	1	−1	0	0.18184	50.3156	0.118
2	1	0	−1	0.21806	56.3425	0.130
3	0	1	1	0.09378	39.0243	0.176
4	−1	0	−1	0.28144	86.2920	0.110
5	0	0	0	0.16874	50.3123	0.095
6	0	1	−1	0.22250	58.3627	0.136
7	0	−1	−1	0.36009	79.6789	0.120
8	1	0	1	0.09550	38.2261	0.145
9	0	0	0	0.16802	50.3121	0.113
10	1	1	0	0.11139	40.6865	0.140
11	−1	0	1	0.11762	50.1745	0.155
12	0	−1	1	0.15066	47.5486	0.120
13	−1	1	0	0.10950	55.0624	0.131
14	0	0	0	0.17708	50.3144	0.103
15	−1	−1	0	0.22825	74.2222	0.106

$$MSE = \frac{\sum_{i=1}^{n} (x_i - y_i)^2}{n} \tag{11}$$

The second performance criterion is the correlation coefficient (R^2). The R^2 varies between −1 and + 1. R^2 close to +1 indicates a strong positive linear relationship between input parameters and output variables [27]. The R^2 coefficient is calculated from this equation:

$$R^2 = 1 - \left(\frac{\sum_{i=1}^{n} (x_i - y_i)^2}{\sum_{i=1}^{n} y_i^2} \right) \tag{12}$$

Several learning algorithms use backpropagation in their processing systems to determine the weights and biases of neural structures. Figure 11 presents the general NNarchitecture with the different parameters.

For structural NN modeling, the Levenberg-Marquardt (LM) algorithm, the scaled conjugate gradient (SCG) algorithm, and the BR algorithm were used. The present work uses the sigmoid function as an activation function in order to normalize the output response. The activation function is represented by the following equation:

$$f(p_i) = \frac{2}{1 + e^{-2p_i}} - 1 \tag{13}$$

where p is the input conversion function.

For all neural architectures, the data are divided into three groups: learning, testing, and validation. Seventy percentage of the data is devoted to the learning phase, 15% to the testing phase, and finally 15% to validation. Table 10 shows how to figure out the best learning algorithm, the number of hidden layers, and the number of best outputs. After several tests, the optimal architecture in this study for a single output is {3-10-1} for the output variable E_{tot} and {3-14-1} for the variables C_{tot} and Ra. The same LM learning algorithm is used to realize all optimal structures. The optimal architecture with three outputs (E_{tot}, C_{tot}, and Ra) is now presented by the {3-10-3} architecture realized with the BR algorithm. The backpropagation algorithm was very good at predicting the amount of energy used, the cost of machining, and the quality of the surface. Figure 12 illustrates the predicted values of E_{tot}, C_{tot}, and Ra compared to the experimental values for the single output

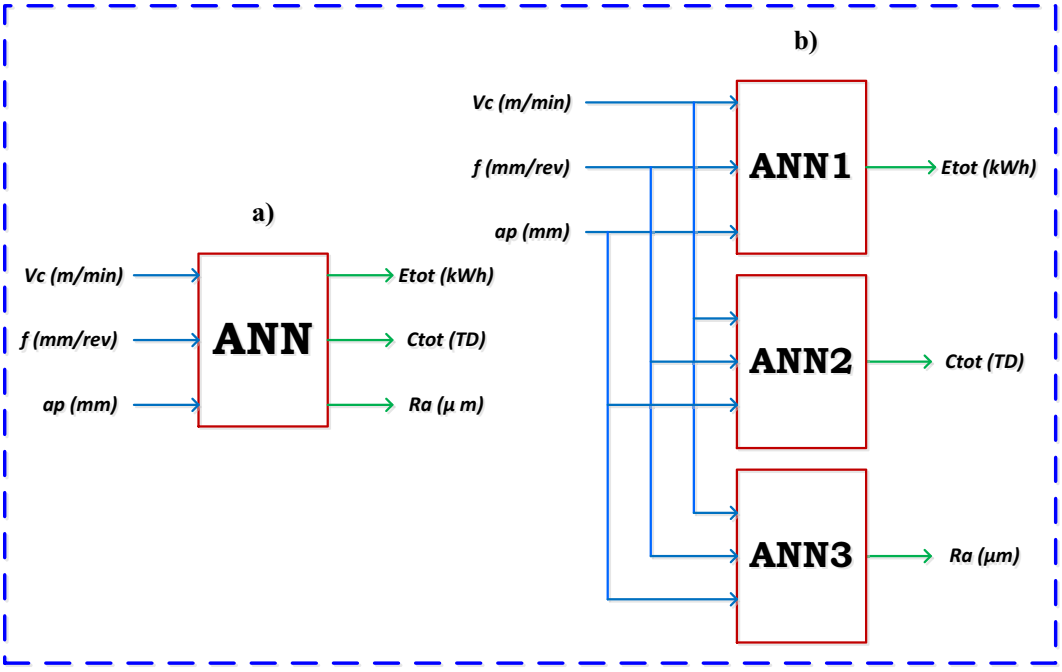

Figure 10. Proposed neural architectures.

https://doi.org/10.1017/S089006042400009X Published online by Cambridge University Press

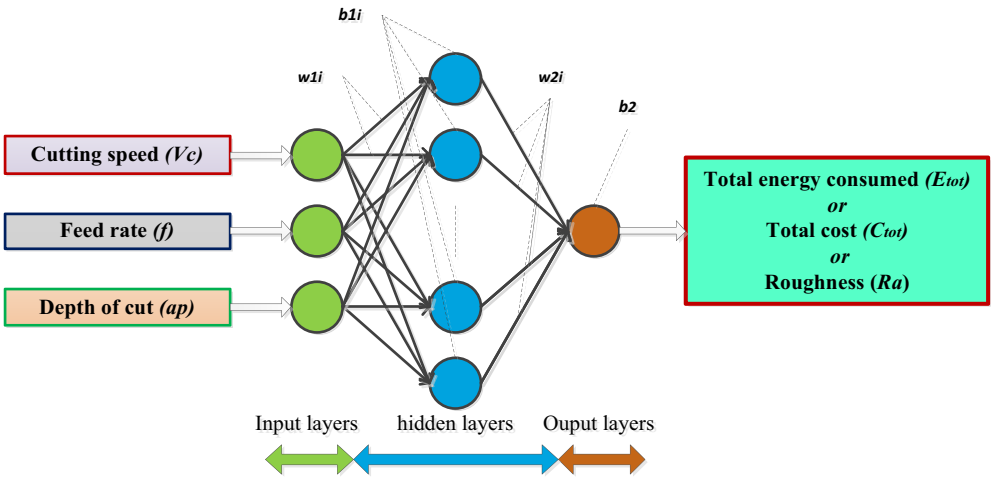

Figure 11. General neural network architecture.

Table 10. Different neural architectures (second case)

Algorithm	ANN	E_{tot}				C_{tot}				Ra			
		MSE		R^2		MSE		R^2		MSE		R^2	
A single output		Train	Test	Train	Test	Train	Test	Train	Test	Train	Test	Train	Test
LM	**3_10_1**	**2.56E–11**	**1.65E–5**	**0.9999**	**0.99**	8.59E–07	2.58	0.99999	1	3.18E–06	8.06E–04	0.996	0.999
LM	**3_14_1**	1.38E–15	1.65E–4	0.9999	0.99	**1.23E–28**	**1.42**	**0.99999**	**0.99**	**2.90E–06**	**2.31E–04**	**0.997**	**1**
BR	3_10_1	4.14E–06	1.38E–3	0.9996	1	7.01E–07	14.04	0.99999	1	1.84E–05	3.28E–04	0.980	0.999
BR	3_14_1	1.97E–08	7.98E–4	0.9999	1	7.01E–07	2.11	0.99999	1	1.59E–05	4.21E–04	0.983	0.999
SCG	3_10_1	3.28E–06	6.80E–4	0.9997	1	4.19E–02	23.94	0.9998	1	1.48E–05	3.53E–04	0.984	1
SCG	3_14_1	4.66E–06	2.94E–2	0.9995	1	2.22E–01	1.74	0.99942	1	5.52E–05	2.70E–04	0.961	1
Three outputs		**MSE_Training**		**MSE_Testing**		**R^2_Training**		**R^2_Testing**					
LM	3_6_3	8.26E–05		74.95E–00		0.99999		0.99999					
LM	3_10_3	1.88E–02		4.97E–02		0.99998		0.99998					
LM	3_12_3	4.51E–00		3.54E–00		0.99723		0.99742					
LM	3_14_3	7.25E–01		2.76E–01		0.99954		0.99999					
BR	3_6_3	8.72E–06		7.44E–00		0.99999		0.99998					
BR	**3_10_3**	**3.57E–06**		**5.49E–03**		**0.99999**		**0.99999**					
BR	3_12_3	7.12E–06		5.62E–00		0.99999		0.99804					
BR	3_14_3	6.96E–06		3.63E–02		0.99999		0.99999					
SCG	3_6_3	6.73E–01		105.83E–00		0.99954		0.99945					
SCG	3_10_3	2.22E–00		30.94E–00		0.99853		0.97474					
SCG	3_12_3	5.65E–02		1.56E–00		0.99996		0.99911					
SCG	3_14_3	46.19E–00		1.37E–00		0.99365		0.99987					

structure. The R^2 for Etot, Ctot, and Ra are 0.9984, 0.9963 and 0.8741, respectively. These values show a good correlation between the predicted values and the experimental values. On the other hand, the MSE for the output responses is low, namely 8.25 10^{-6} (kWh), 1.42 TD (0.44 $), and 1.17 10^{-4} µm, respectively, for E_{tot}, C_{tot}, and Ra. Figure 13 shows the predicted values of Etot, Ctot, and Ra versus the experimental values for the three-lead structure. The R^2 for Etot, Ctot, and Ra are 0.9992, 1, and 0.9117 respectively. So, from Table 10 and Figures 12 and 13, the conclusion is drawn that the LM algorithm has good learning with a single output response. On the other hand, the BR algorithm has good learning with a multi-criteria response (three for this work). By comparison between these architectures, the {3-10-3} architecture with the BR algorithm has a good correlation compared to the other architectures. The MSE global MSE for this architecture is 2.74 10^{-3}. Therefore, the use of artificial intelligence by neural networks seems

https://doi.org/10.1017/S089006042400009X Published online by Cambridge University Press

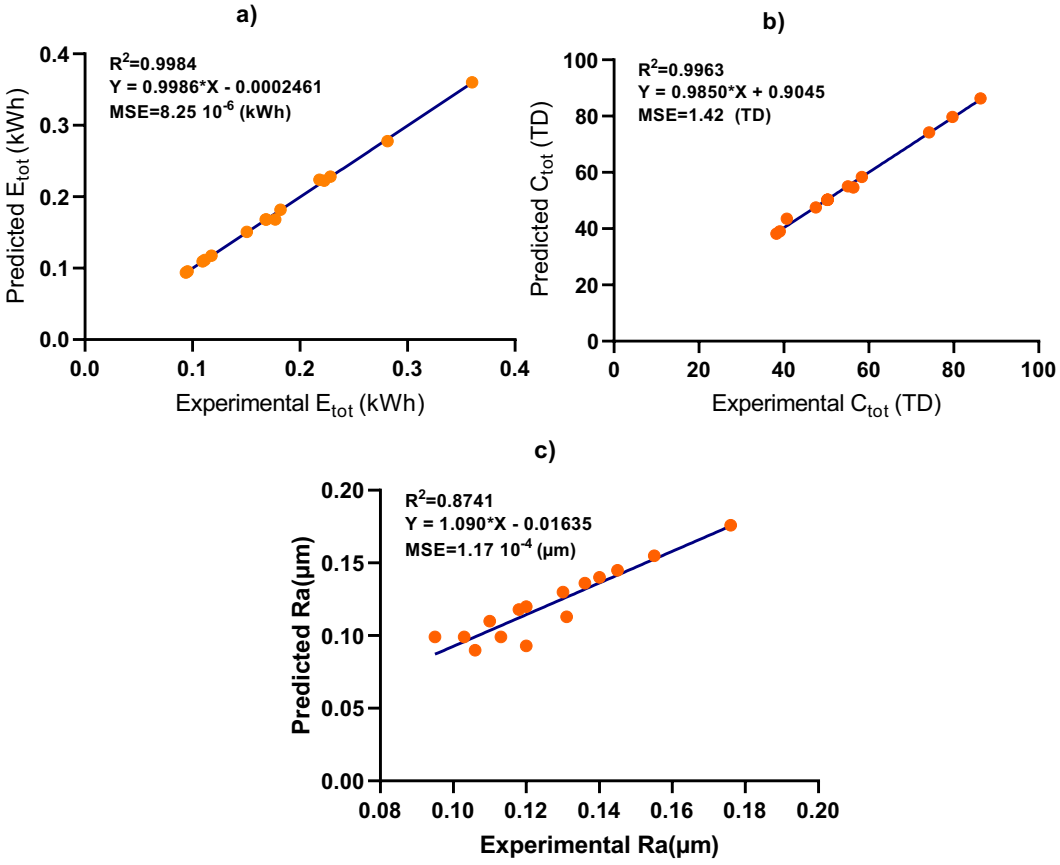

Figure 12. Experimental values versus predicted values (single output: {3-10-1} and {3-14-1}).

to be a useful methodology to simulate multi-criteria responses in mechanical manufacturing. In what follows, the {3-10-3} architecture will be retained.

Prediction with ANFIS model

The ANFIS model is highlighted to predict experimental results in different fields of engineering [28, 29 and 30]. ANFIS is a hybrid fuzzy inference approach from Sugeno [31] which simultaneously combines a fuzzy inference system (FIS) with a NN. This combination aims to make the system efficient in order to solve complex problems [32]. In the general case, the ANFIS model includes five consecutive treatment lines. The lines (layers) are connected to each other by different nodes. Each entry node is drawn from the previous line. Figure 14 presents the general architecture of the ANFIS model. The numerical interpretation of this architecture can be presented as follows:

Rule 1 = if x is A_1 and y is B_1, then $f_1 = p_1 x + q_1 y + r_1$

Rule 2 = if x is A_2 and y is B_2, then $f_2 = p_2 x + q_2 y + r_2$

where x and y are the input parameters of the experimental study, and p_i and q_i represent the variables of the fuzzy set. The output function of the ANFIS model is presented by

$$f = \bar{w}_1 f_1 + \bar{w}_2 f_2 \tag{14}$$

where $\bar{w}_1 = \frac{w_1}{w_1 + w_2}$; $\bar{w}_2 = \frac{w_2}{w_1 + w_2}$

where w_i is the trigger strength for each rule.

In this present work, in order to find the optimal architecture of the ANFIS model, a combination of numbers and types of membership functions (MFs) (Gaussian-shaped MFs, gaussmf and gauss2mf, and triangular-shaped MF, trimf) was carried out. The MFs used in this work are the trimf, gaussmf, and gauss2mf. The numbers of MF used are {2 2 2}, {2 2 3}, and {2 3 3}. The MF of constant and linear types is used for the output variables. The ANFIS modeling process runs with 75% of the data for training and 25% for testing. In this process, the iteration number for the mapping is equal to 100. Table 11 presents the different combinations of ANFIS architecture with the different MFs. According to this table, structure {2 2 2} is the optimal structure for the three output responses (E_{tot}, C_{tot}, and Ra). According to the results, the function (trimf) has the lowest test error for the energy consumed (E_{tot}) with a linear output. On the other hand, the (gaussmf) function has the lowest error for C_{tot} and Ra output responses with constant and linear output functions, respectively. The MSE_All values for the E_{tot}, C_{tot}, and Ra output responses are 0.01913, 3.399 and 4.516 E-3, respectively. Figure 15 illustrates the final {2 2 2} architecture for the three output variables. Figure 16 illustrates the comparison between predicted and experimental values for output responses. The R^2 values for the variables E_{tot}, C_{tot}, and Ra are 0.95, 0.965 and 0.968, respectively. These values present a good correlation but are less weak than those of the neural network, except for the surface quality for the ANFIS model, which is greater than that of the ANN (0.968 > 0.9117). Table 12 shows a comparison between the two ANN and ANFIS models' global MSEs (training and testing) for the different output variables. The result shows that the global MSE of the {3-10-3} neural structure is lower compared

https://doi.org/10.1017/S089006042400009X Published online by Cambridge University Press

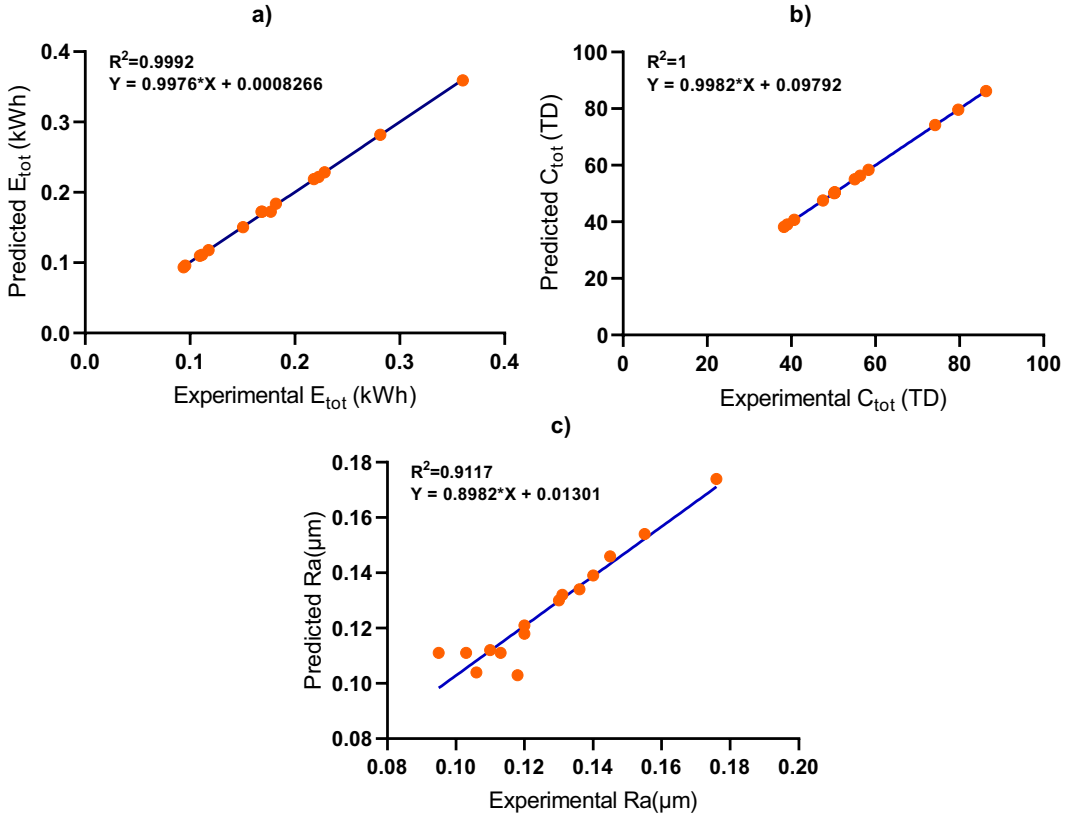

Figure 13. Experimental values versus predicted values (three outputs: {3-10-3}).

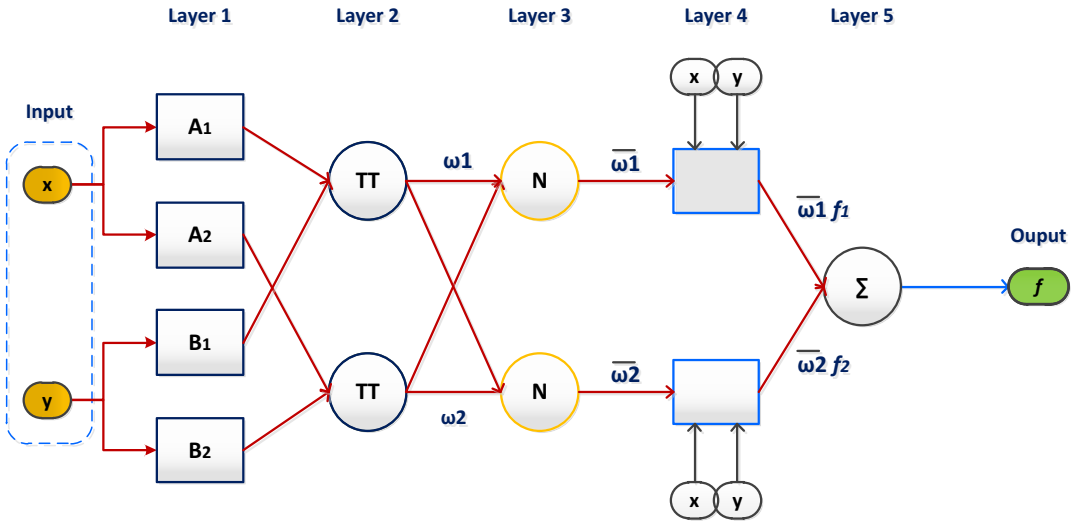

Figure 14. General architecture of the ANFIS model.

to that of the ANFIS model. Indeed, Figures 12 and 13 (ANN), Figures 15 and 16 (ANFIS), and comparison Table 12 show that the use of the BR algorithm with a multi-criteria output response can give good results when compared with ANFIS.

A 3D surface plot study was carried out in order to describe the effects of the cutting parameters on the output responses. Figure 17 shows the variation of energy consumed (E_{tot}), cost (C_{tot}), and surface quality as a function of the cutting parameters. Figure 17a and 17b shows that for a decrease in the feed rate (f), there is an increase in the energy (E_{tot}) and the cost (C_{tot}). This conclusion is because the machining time decreases when the feed rate increases, which positively influences the energy consumption and the cost. This conclusion is similar to the studies of references [33, 34 and 35]. Figure 17e shows that as the feed rate increases, the surface quality decreases. In other words, the roughness (Ra) increases. Indeed, the feed rate (f) has a remarkable influence on the surface quality compared with the cutting speed. In this present work, the depth of cut (a_p) is chosen so that all levels have the same depth of

https://doi.org/10.1017/S089006042400009X Published online by Cambridge University Press

Table 11. Different combinations of ANFIS architecture (second case)

N°	MF	Function	Output Function	MSE					
				E_{tot}		C_{tot}		Ra	
				Training	**Testing**	**Training**	**Testing**	**Training**	**Testing**
1	2 2 2	trimf	Constant	7.8416 E–3	0.05540	1.1554	5.7004	0.011449	0.02187
2	**2 2 2**	**trimf**	**Linear**	**1.4493 E–4**	**0.03812**	1.7851 E–4	6.1249	3.674 E–3	5.775 E–3
3	**2 2 2**	**gaussmf**	**Constant**	0.013354	0.07664	**1.1380**	**5.6612**	0.011222	0.02076
4	**2 2 2**	**gaussmf**	**Linear**	1.4493 E–4	0.04799	1.9405 E–4	7.9327	**3.674 E–3**	**4.516 E–3**
5	2 2 3	trimf	Constant	1.2314 E–3	0.08307	0.24543	10.763	4.378 E–3	0.03362
6	2 2 3	trimf	Linear	1.4493 E–4	0.04688	6.6776 E–5	22.323	3.674 E–3	0.04732
7	2 2 3	gaussmf	Constant	1.8205 E–3	0.08021	0.71613	9.7418	4.378 E–3	0.03288
8	2 2 3	gaussmf	Linear	1.4493 E–4	0.04290	4.1635 E–5	26.535	3.674 E–3	0.05488
9	2 3 3	trimf	Constant	1.4493 E–4	0.10174	7.881 E–5	47.256	3.674 E–3	0.064204
10	2 3 3	trimf	Linear	1.4493 E–4	0.12681	4.9551 E–6	47.828	3.674 E–3	0.08988
11	2 3 3	gaussmf	Constant	1.4493 E–4	0.06475	8.5646 E–5	34.968	3.674 E–3	0.05383
12	2 3 3	gaussmf	Linear	1.4493 E–4	0.10273	9.1918 E–6	36.018	3.674 E–3	0.05890

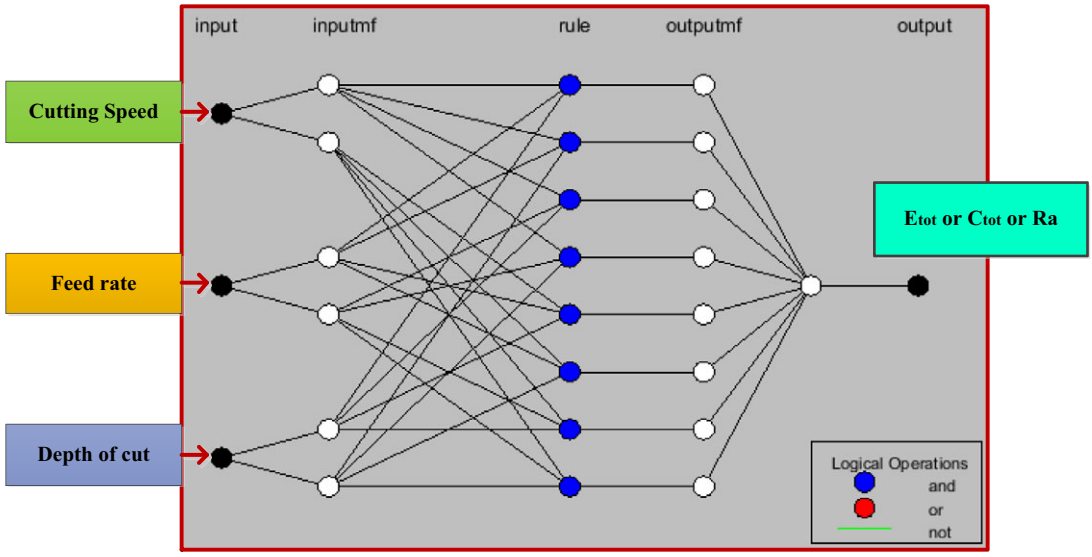

Figure 15. Final {2 2 2} architecture.

cut for a height of cut h. Figures 17(b) and (d) clearly show that as the depth of cut increases, so does the energy (E_{tot}) and the cost (C_{tot}). The decrease in the number of cutting levels, caused by an increase in the depth of cut, leads to a reduction in total machining time. Similarly, for the surface quality, the increase in the depth of cut has a negative influence on the roughness (Ra) (Figure 17(f)). This is because the tool tends to vibrate more as the depth of cut gets deeper, especially if the diameter of the tool is small. These conclusions converge with the studies of Khan Aqib et al. [35], Eser et al. [36] and Devarajaiah et al. [37].

Development of an intelligent simulator based on prediction models ANN and ANFIS

An interactive interface has been developed to help machinists predict the energy consumed, surface quality, and cost of a 2017A alloy part containing an interacting pocket and groove. The simulator was implemented using the "Guide" interface of the MATLAB 2016 software. Figure 18 shows this user interface named "QCE_Intelligent_simulator," which is simple and extremely easy to learn. As shown in the figure, the user must first input the values of the cutting parameters (Inputs), that is, the cutting speed (V_c), the feed rate (f), and the depth of cut (a_p). Subsequently, the user has the choice to predict the results according to the ANN model or the ANFIS model by pressing the "Predict" button.

The Catia-machine interaction is achieved through the production of a G-code program according to the ISO 6983 standard compatible with the CNC director Num of the machining center. The power is measured in real time during the execution of the machining operation. The actual results are compared to what was expected after the data and results have been analyzed [38, 39]. When another operation is executed, the machining parameters are updated.

https://doi.org/10.1017/S089006042400009X Published online by Cambridge University Press

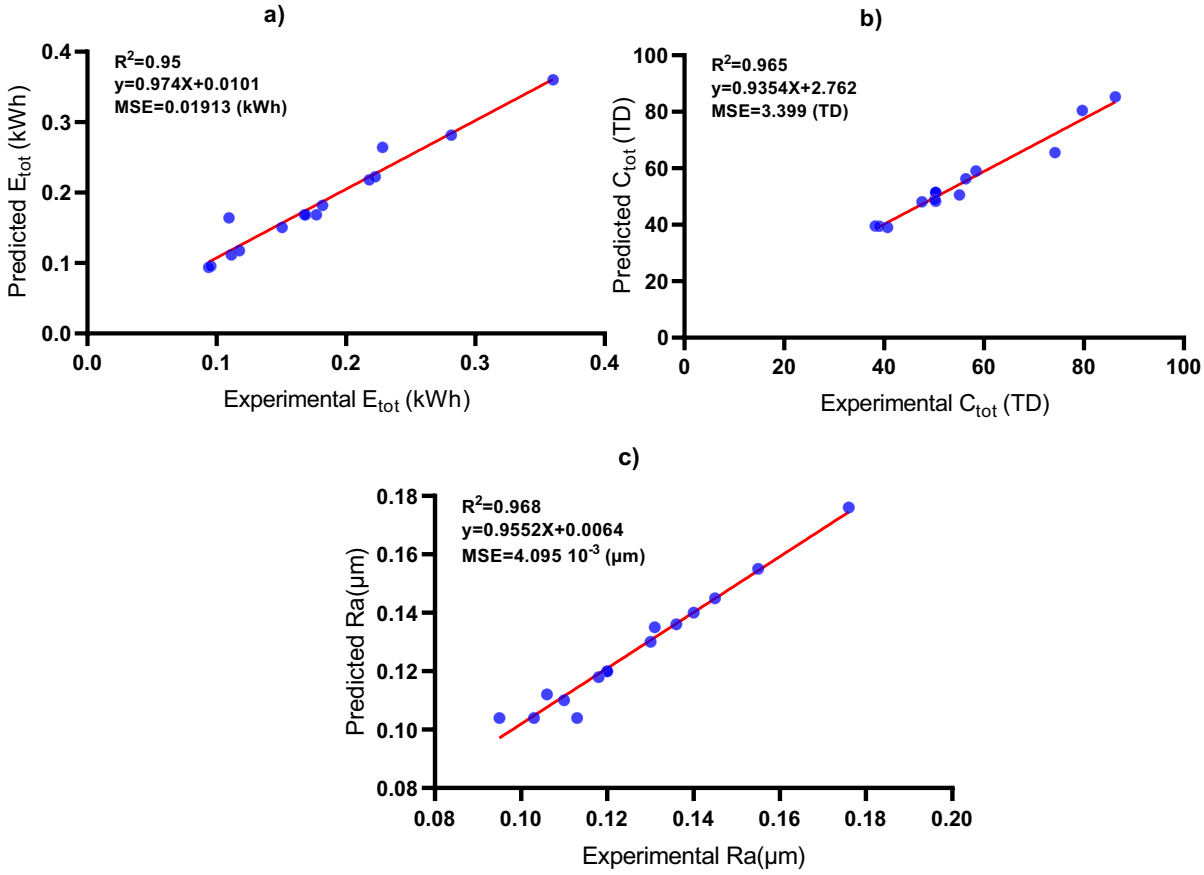

Figure 16. Experimental values versus predicted values (ANFIS model).

Table 12. The MSE_ALL values of the ANN and ANFIS models (second case)

Model	MSE_ALL		
	E_{tot}	C_{tot}	Ra
ANN (3–10–3)	←---------- -2.74×10^{-3} ----------→		
ANFIS (2 2 2)	0.01913	3.399	$4.095\ 10^{-3}$

Comparative analysis

A very few of the researchers have applied artificial intelligence models (ANN and ANFIS) to optimize machining performance in milling. We cite, as examples, works somewhat close to our study: Pourmostaghimi et al. [40] propose a model-based smart optimization methodology to optimize the production cost and material removal rate under surface quality constraint during a turning operation in hardened AISI D2. They determine the optimal machining parameters by applying the particle swarm optimization (PSO) algorithm. Namlu et al. [41] developed an ANN model in the Python programming environment to predict the cutting forces of Ti–6Al–4 V machining. The results showed that the experimental cutting forces were estimated with a successful prediction rate of 0.99 with mean absolute percentage error and root MSE of 1.85% and 13.1, respectively. Pourmostaghimi et al. [42] proposed a novel PSO-RDNN hybrid approach combining PSO algorithm with recurrent dynamic neural network (RDNN), for multi-performance optimization of machining parameters in finishing turning of AISI D2 hardened parts. The proposed methodology returns a Pareto optimality plot, which represents cutting variables optimized for several different cutting conditions.

The work of Sada and Ikpeseni [43] is the only research closest to our work and which can be compared with the results of our work even if the materials are not the same. Sada and Ikpeseni provide valuable insights into the predictive performance of ANNs and ANFISs for predicting the machining performance of AISI 1050 steel. This study focuses on a specific application and evaluates the modeling ability of both ANN and ANFIS models. In this research, the authors likely conducted experiments or collected data related to the machining process of AISI 1050 steel. They then compared the predictive capabilities of ANN and ANFIS models by training and testing them on the collected data. The evaluation criteria could include accuracy, precision, recall, mean absolute error, or other relevant performance metrics. Sada and Ikpeseni assess the performance of ANN and ANFIS models in predicting machining responses (metal removal rate and tool wear) in an AIS steel turning operation. The R^2 obtained from the analysis further confirms the preference of ANN with a maximum value of 92.1% recorded using ANN compared to that of ANFIS of 73%. Based on their analysis and comparison, the authors found that the NN models (ANN) exhibited superior predictive performance over the ANFIS models. This conclusion aligns with your statement that the authors of reference [43] established the predictive superiority of neural networks over ANFIS. The study's findings suggest that ANN models were better at capturing the intricate relationships and patterns in the machining performance data of AISI 1050 steel. These NN

https://doi.org/10.1017/S089006042400009X Published online by Cambridge University Press

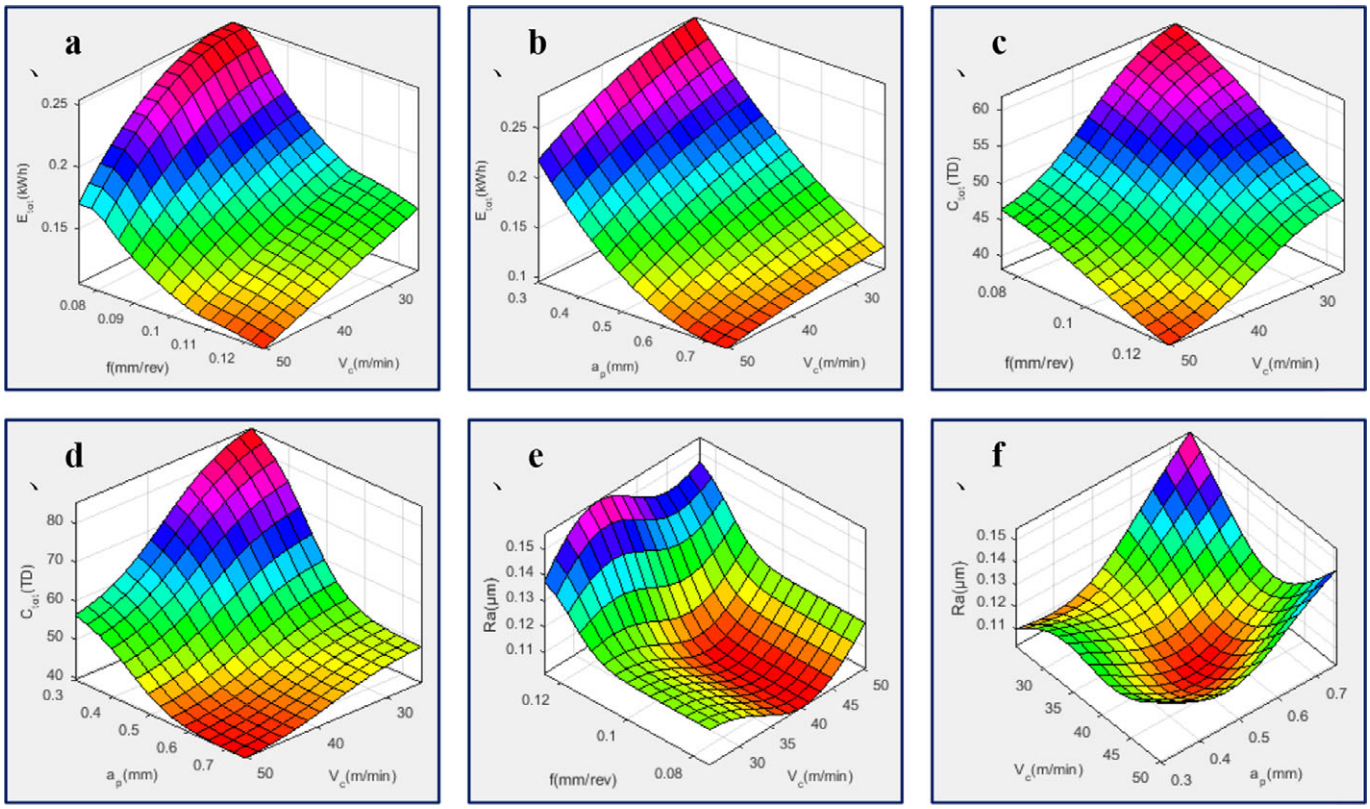

Figure 17. 3D surface plot of energy (E_{tot}), cost (C_{tot}), and roughness (Ra).

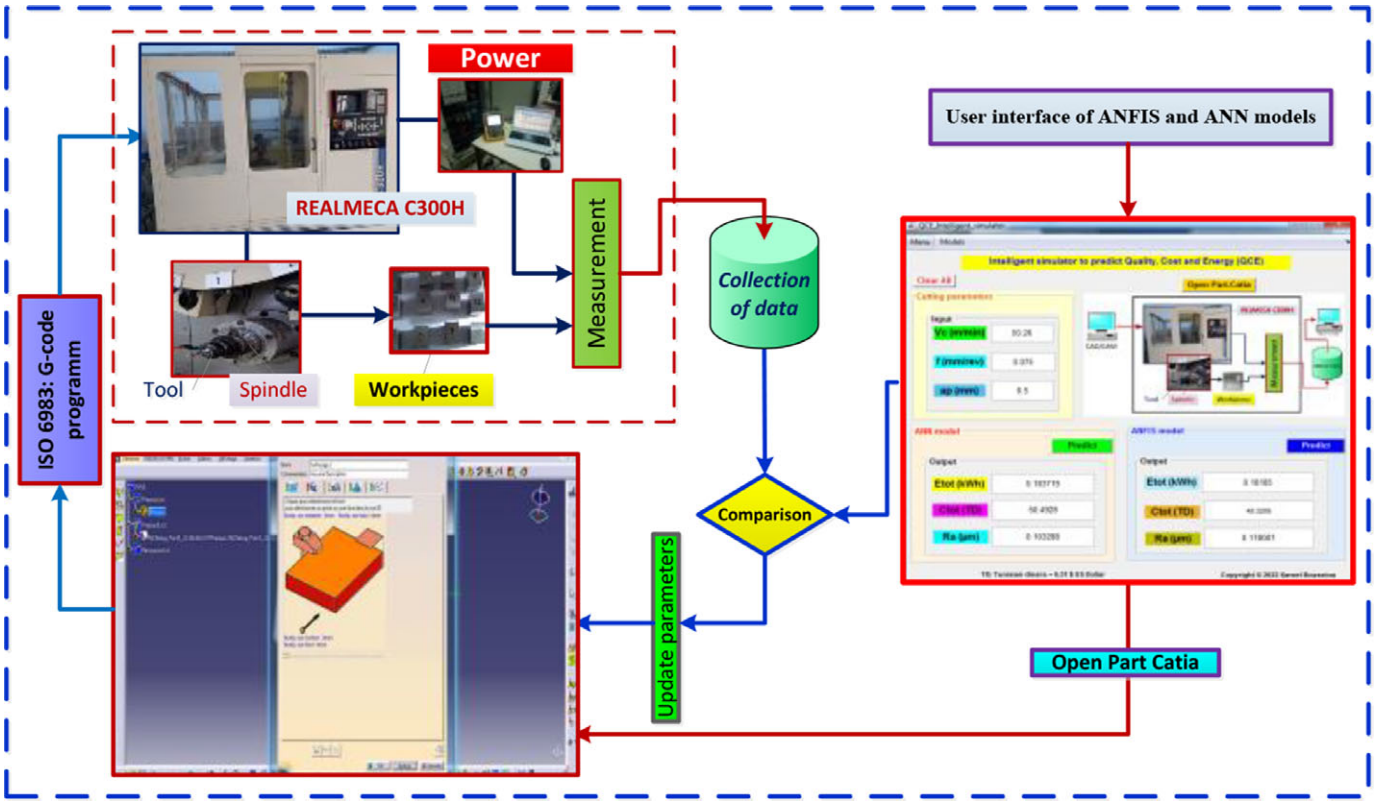

Figure 18. QCE_Intelligent_simulator.

https://doi.org/10.1017/S089006042400009X Published online by Cambridge University Press

models likely outperformed ANFIS models in terms of accuracy and generalization capability.

In our work, we obtained the R^2 values for E_{tot}, C_{tot}, and Ra: 99.92%, 100%, and 91.17%, respectively, for the ANN model and 95%, 96.5%, and 96.8%, respectively, for the ANFIS model. In our article, we observed a strong correlation between the results, highlighting the superiority of the ANN model over the ANFIS model in all instances, which aligns with the findings of Sada and Ikpeseni [43].

The obtained R_2 in your work demonstrate the superior predictive performance of the ANN model compared to the ANFIS model for the variables E_{tot}, C_{tot}, and Ra. The high R^2 values achieved by the ANN model, such as 99.92% for E_{tot}, 100% for C_{tot}, and 91.17% for Ra, indicate a strong correlation between the predicted values and the actual values. The superior predictive performance of the ANN model compared to the ANFIS model, as evidenced by the high R_2 obtained in our work, can be attributed to several scientific factors. NNs, including ANNs, excel at capturing and representing nonlinear relationships in data due to their flexible and adaptable nature. They can adjust their internal parameters during training, optimizing their performance and enabling them to model complex nonlinear dependencies more effectively than ANFIS models. Additionally, the end-to-end learning capability of neural networks allows them to learn directly from raw input data without manual feature engineering, extracting relevant features and uncovering hidden patterns. The scalability and depth of neural networks, particularly in deep architectures, enable them to handle intricate and high-dimensional datasets, contributing to their superior predictive power. These scientific factors collectively justify the superior predictive performance of the ANN model in our work.

Conclusion

The increase in the world's population promotes an increased demand for products, which requires enormous energy consumption in industries. In order to evaluate the trade-offs between cut quality, manufacturing cost, and energy consumption (QCE). This article presents an approach that integrates ANNs and ANFIS to predict the effects of strategies, machining sequences, and cutting parameters on the consumption of energy, machining cost, and Ra. Two in-depth case studies were carried out to understand the effects of the parameters introduced into the multi-criteria output responses. Based on the results already found, the studies first show that the strategies and the planning of the machining sequences have a remarkable influence on the energy consumption, the cost of machining, and the surface quality of the parts. In this work, a multi-objective optimization based on the GRA was proposed, which is applied to optimize the sequences and strategies of machining on a part that contains interacting entities. The results obtained confirm that the proposed optimization method is a very indispensable tool for multi-criteria optimization. The use of a variety of architectures and a variety of learning algorithms for the construction of neural networks allows us to increase the range of choice and the rigorous selection of the optimal solution (architecture + algorithm). The {3-10-3} architecture with the BR algorithm is the optimal neural architecture that yields an overall MSE of 2.74×10^{-3}. Similarly, for the ANFIS, the optimal structure which gives a better error and better correlation is the {2 2 2} structure, and this for the three output variables (E_{tot}, C_{tot}, and Ra). Studies also show that for a decrease in the forward speed (f), there is an increase in E_{tot} and C_{tot}. In contrast to energy and cost, a decrease in *f* causes a decrease in Ra.

Future work will aim to extend multi-criteria output responses to account for other factors (e.g., dimensional error and vibration). Finally, an application to a wider range of prediction and optimization with other methods of artificial intelligence can contribute positively to the desired performance.

Nomenclature

N	Spindle speed (rev/min) (rpm)
V_c	Cutting speed (m/min)
f	Feed rate (mm/rev)
a_e	Cutting width (mm)
P_{pi}	Total power consumed for machining the pocket for a cutting width = tool diameter (layer i) (W)
P_{c_pi}	Power cutting for machining the pocket for a cutting width = tool diameter (layer i) (W)
P_0	No-load power (W)
P_g	Total power consumed for machining the groove (W)
P_{c_g}	Power cutting for machining the groove (W)
P^*_{pi}	Total power consumed for machining the pocket for a cutting width = a_e (layer i) (W)
$P^*_{c\_pi}$	Power cutting for machining the pocket for a cutting width = a_e (layer i) (W)
a_p	Depth of cut (mm)
V_f	Feed rate (mm/min)
P_c	The power consumed (W)
$C_{Machine}$	Machine cost (TD)
C_{Tool}	Tool cost (TD)
C_{Energy}	Energy cost (TD)
μ_1	Cost of assembly and adjustment (TD)
μ_2	Machine cost per hour (TD/h)
ε	Cost of a cutting edge and tool change (TD)
δ	Energy cost (TD/kWh)
TD	Tunisian dinars = 0.31 $ US Dollar
t_c	Cutting time (s)
t_{cycle}	Cycle time (s)
ANN	Artificial neurons networks
$ANFIS$	Adaptive neuro-fuzzy inference systems
GRA	Gray relational analysis

Acknowledgements. The authors would like to thank the workshop team of the Higher Institute of Technological Studies of Gabes for their advice and support during this work.

Funding statement. Not applicable.

Competing interest. The authors declare that they have no conflict of interest.

References

[1] **Ben Yahia N, Fnaiech F, Abid S and Hadj S B.** (2002) Manufacturing Process Planning Application using Artificial Neural Networks. *IEEE International Conference on Systems, Man and Cybernetics* **7**.

[2] **Girish K and Kuldip S S.** (2015) Predictive Modelling and Optimization of Machining Parameters to Minimize Surface Roughness using Artificial Neural Network Coupled with Genetic Algorithm. *Procedia CIRP* **31**: 453–458, DOI: 10.1016/j.procir.2015.03.043

[3] **Aykut E, Elmas A, kar A, Mustafa A and Fuat K.** (2021) Artificial Intelligence-Based Surface Roughness Estimation Modelling for Milling of AA6061 Alloy. *Advances in Materials Science and Engineering*, DOI: 10.1155/2021/5576600

4] **Serra R, Chibane H and Duchosal A.** (2018) Multi-objective optimization of cutting parameters for turning AISI 52100 hardened steel. *The*

https://doi.org/10.1017/S089006042400009X Published online by Cambridge University Press

International Journal of Advanced Manufacturing Technology **99**: 2025–2034, DOI: 10.1007/s00170-018-2373-3

5] **Tzu-Liang T**, **Konadaa U and Yongjin K.** (2016) A novel approach to predict surface roughness in machining operations using fuzzy set theory. *Journal of Computational Design and Engineering* **3**:1–13, DOI: 10.1016/j.jcde.2015.04.002

[6] **Bousnina K. and Hamza A.**, (2020) Reducing The Energy Consumed And Increasing Energy Efficiency In The Turning Process. *International Journal of Modern Manufacturing Technologies*; **12**(2), 23–28.

[7] **Yansong G**, **Jef L**, **Joost D and Bert L.** (2012) Optimization of energy consumption and surface quality in finish turning. *Procedia CIRP* **1**: 512–517, DOI:10.1016/j.procir.2012.04.091

[8] **Ampara A and Paul T M.** (2014) Critical factors in energy demand modelling for CNC milling and impact of toolpath strategy. *Journal of Cleaner Production* **78**:63–74, DOI:10.1016/j.jclepro.2014.04.065

[9] **Resul S. A**, **Müge K and Hakkı Ö Ü**. (2016) Modelling and optimization of energy consumption for feature based milling. *Int J Adv Manuf Technol* **86**: 3345–3363,. DOI: 10.1007/s00170-016-8441-7

[10] **Congbo L**, **Lingling L**, **Ying T**, **Qian Y and Yantao Z.** (2016) Operational Strategies for Energy Efficiency Improvement of CNC Machining. *International Conference on Automation Science and Engineering*,. DOI: 10.1109/COASE.2016.7743553

[11] **Qiulian W**, **Fei L and Xianglian W.** (2014) Multi-objective optimization of machining parameters considering energy consumption. *Int J Adv Manuf Technol* **71**:1133–1142, DOI: 10.1007/s00170-013-5547-z

[12] **Congbo L**, **Xingzheng C**, **Ying T and Li L.** (2017) Selection of optimum parameters in multi-pass face milling for maximum energy efficiency and minimum production cost. *Journal of Cleaner Production* **140**(3): 1805–1818, DOI: 10.1016/j.jclepro.2016.07.086

[13] **Yongmao X**, **Zhigang J**, **Quan G**, **Wei Y and Ruping W.** (2021) A novel approach to CNC machining center processing parameters optimization considering energy-saving and low-cost. *Journal of Manufacturing Systems* **59**:535–548. DOI: 10.1016/j.jmsy.2021.03.023

[14] **Perez H**, **Diez E**, **Perez J and Vizan A.** (2013) Analysis of machining strategies for Peripheral milling." *Procedia Engineering* **63**:573–581, DOI: 10.1016/j.proeng.2013.08.193

[15] **Sen J**, **Yingguang L and Changqin, L.** (2018) A non-uniform allowance allocation method based on interim state stiffness of machining features for NC programming of structural parts. *Visual Computing for Industry, Biomedicine and Art* **1**(4), DOI: 10.1186/s42492-018-0005-2

[16] **Kutschenreiter I P.** (2008) Application of artificial neural network for determination of standard time in machining. *J Intell Manuf* **19**:233–240, DOI: 10.1007/s10845-008-0076-6

[17] **Edem Isuamfon F.**, **Vincent A. Balogun, and Paul T. Mativenga**. (2017) An investigation on the impact of tool path strategies and machine tool axes configurations on electrical energy demand in mechanical machining. *The International Journal of Advanced Manufacturing Technology* **92**.5: 2503–2509. DOI:10.1007/s00170-017-0342-x

[18] **Altıntaş Resul S**, **Müge K, and Hakkı Özgür Ü**. (2016) Modelling and optimization of energy consumption for feature based milling. *The International Journal of Advanced Manufacturing Technology* **86**.9: 3345–3363. DOI:10.1007/s00170-016-8441-7

[19] **Zaleski K**, **Jakub M, and Andrzej Z.** (2020) Highly efficient milling on the example of selected machining strategies. *Advances in Science and Technology. Research Journal* **14**.1. DOI:10.12913/22998624/116356

[20] **Ali Raneen Abd**, et al. (2019) Multi-response optimization of face milling performance considering tool path strategies in machining of Al-2024. *Materials* **12**.7: 1013. DOI:10.3390/ma12071013

[21] **Aramcharoen A, and Paul T. M.** (2014) Critical factors in energy demand modelling for CNC milling and impact of toolpath strategy. *Journal of Cleaner Production* **78**: 63–74. DOI:10.1016/j.jclepro.2014.04.065

[22] **Kant G, and Kuldip Singh S.** (2014) Prediction and optimization of machining parameters for minimizing power consumption and surface roughness in machining. *Journal of Cleaner Production* **83**: 151–164. DOI: 10.1016/j.jclepro.2014.07.073

[23] **Kumar R**, **Paramjit Singh B, and Sehijpal S.** (2017) Multi objective optimization using different methods of assigning weights to energy consumption responses, surface roughness and material removal rate during rough turning operation. *Journal of Cleaner Production* **164**: 45–57. DOI:10.1016/j.jclepro.2017.06.077

[24] **Çay Y**, et al. (2013) Prediction of engine performance and exhaust emissions for gasoline and methanol using artificial neural network. *Energy* **50**: 177–186. DOI:10.1016/j.energy.2012.10.052

[25] **Vaishna, S**, **Ankit A, and Desai K. A.** (2020) Machine learning-based instantaneous cutting force model for end milling operation. *Journal of Intelligent Manufacturing* **31**.6: 1353–1366. DOI:10.1007/s10845-019-01514-8

[26] **Najafi G.**, et al. (2009) Performance and exhaust emissions of a gasoline engine with ethanol blended gasoline fuels using artificial neural network. *Applied energy* **86**.5: 630–639. DOI:10.1016/j.apenergy.2008.09.017

[27] **Sayin C**, et al. (2007) Performance and exhaust emissions of a gasoline engine using artificial neural network. *Applied thermal engineering* **27**.1: 46–54. DOI:10.1016/j.applthermaleng.2006.05.016

[28] **Toghroli A.** et al. (2014) Prediction of shear capacity of channel shear connectors using the ANFIS model. *Steel Compos Struct* **17**.5: 623–639. DOI:10.12989/scs.2014.17.5.000

[29] **Sedghi Y.** et al. (2018) Application of ANFIS technique on performance of C and L shaped angle shear connectors. *Smart structures and systems* **22**.3: 335–340.

[30] **Zhou J.** et al. (2021) Performance evaluation of hybrid FFA-ANFIS and GA-ANFIS models to predict particle size distribution of a muck-pile after blasting. *Engineering with computers* **37**.1: 265–274. DOI:10.1007/s00366-019-00822-0

[31] **Mandal S.** et al. (2018) ANFIS based model to forecast the Wire-EDM parameters for machining an Ultra High Temperature Ceramic composite. *IOP Conference Series: Materials Science and Engineering*. Vol. **377**. No. 1. IOP Publishing, DOI:10.1088/1757-899X/377/1/012088

[32] **Saw Lip H.** et al. (2018) Sensitivity analysis of drill wear and optimization using Adaptive Neuro fuzzy–genetic algorithm technique toward sustainable machining. *Journal of Cleaner Production* **172**: 3289–3298. DOI: 10.1016/j.jclepro.2017.10.303

[33] **Bagaber Salem A, and Ahmed Razlan Y.** (2017) Multi-objective optimization of cutting parameters to minimize power consumption in dry turning of stainless steel 316. *Journal of cleaner production* **157**: 30–46. DOI:10.1016/j.jclepro.2017.03.231

[34] **Li Congbo**, et al. (2019) A comprehensive approach to parameters optimization of energy-aware CNC milling. *Journal of Intelligent Manufacturing* **30**.1 123–138. DOI:10.1007/s10845-016-1233-y

[35] **Khan Aqib M.** et al. (2019) Multi-objective optimization of energy consumption and surface quality in nanofluid SQCL assisted face milling. *Energies* **12**.4: 710. DOI:10.3390/en12040710

[36] **Eser A.** et al. (2021) Artificial intelligence-based surface roughness estimation modelling for milling of AA6061 alloy. *Advances in Materials Science and Engineering*. DOI:10.1155/2021/5576600

[37] **Devarajaiah, D., and Muthumari, C.** (2019) Fuzzy logic-integrated PSO methodology for parameters optimization in end milling of Al/SiCp MMC. *Journal of the Brazilian Society of Mechanical Sciences and Engineering*, **41**(5), 1–12. DOI: 10.1007/s40430-019-1725-8

[38] **Bousnina, K.**, **Hamza, A.**, **Yahia, N. B.** (2022) Energy Optimization for Milling 304L Steel using Artificial Intelligence Methods. *International Journal of Automotive and Mechanical Engineering*, **19**(3), 9928–9938. DOI: 10.15282/ijame.19.3.2022.05.0765

[39] **Bousnina K.**, **Hamza A**, **Ben Yahia N.** (2022) An approach to the influence of the machining process on power consumption and surface quality during the milling of 304L austenitic stainless steel. *Journal of Mechanical Engineering and Sciences*, **16**(3), 9093–9109. DOI: 10.15282/jmes.16.3.2022.11.0720

[40] **Pourmostaghimi, V.**, **Zadshakoyan, M.**, & **Badamchizadeh, M.** (2020). Intelligent model-based optimization of cutting parameters for high quality turning of hardened AISI D2. *Artificial Intelligence for Engineering Design, Analysis and Manufacturing*, **34**(3), 421–429. DOI:10.1017/S089006041900043X

[41] **Namlu, R.**, **Turhan, C.**, **Sadigh, B.**, & **Kılıç, S.** (2021). Cutting force prediction in ultrasonic-assisted milling of Ti–6Al–4V with different machining conditions using artificial neural network. *Artificial Intelligence*

https://doi.org/10.1017/S089006042400009X Published online by Cambridge University Press

for Engineering Design, Analysis and Manufacturing, **35**(1), 37–48. DOI: 10.1017/S0890060420000360

[42] **Pourmostaghimi, V.**, **Zadshakoyan, M.**, **Khalilpourazary, S.**, & **Badamchizadeh, M.** (2022). A hybrid particle swarm optimization and recurrent dynamic neural network for multi-performance optimization of hard turning operation. *Artificial Intelligence for Engineering Design, Analysis and Manufacturing*, **36**, E28. DOI: 10.1017/S0890060422000087

[43] **Sada SO**, **Ikpeseni SC**. (2021) Evaluation of ANN and ANFIS modeling ability in the prediction of AISI 1050 steel machining performance. *Heliyon*, **7**(2):e06136. DOI: 10.1016/j.heliyon.2021.e06136. PMID: 33553780; PMCID: PMC7856477.

https://doi.org/10.1017/S089006042400009X Published online by Cambridge University Press